



Design and characterization of the lateral actuator of a bimodal tactile display with two excitation directions[☆]

Andreas S. Schmelt^{a,*}, Viktor Hofmann^a, Eike C. Fischer^b, Marc C. Wurz^b, Jens Twiefel^a

^a Institute of Dynamics and Vibration Research, Leibniz University Hannover, Appelstraße 11, Hannover, Germany

^b Institute of Micro Production Technology, Leibniz University Hannover, An der Universitaet 2, Garbsen, Germany

ARTICLE INFO

Keywords:

Tactile display
Load model
Piezoelectric
Bimorph
Perception threshold

ABSTRACT

In this paper, a bimodal tactile display used to stimulate the mechanoreceptors is proposed. The use of tactile displays to provide tactile sensations has become the object of increasing interest in recent years. Most of these displays have only one actuator type to generate the tactile perceptions and the spatial resolution of many displays is too rough for good tactile impression. Hence, for the proposed tactile display, two types of actuators for lateral and vertical (normal) excitation are combined. The resolution of the 4×4 array is 2.4 mm. Due to its design concept, the presented display is easily expanded. The normal actuator is based on the reluctance principle and the lateral actuator is based on the piezoelectric effect. This contribution focuses on the design and characterization of the piezoelectric actuator. The lateral actuator is mounted on the normal actuator. This has a significant impact on the design of the piezoelectric actuator. To describe the dynamics of this actuator, a Transfer Matrix Method (TMM) Model is created. The mechanical boundary condition at the connection to the normal actuator is included utilizing discrete elements. The model is validated by experiments. Using the model, the geometry of the actuator elements is designed. For performance tests, several experiments have been carried out. The behavior of the lateral actuator has been analyzed in the two end positions of the normal actuators for different load conditions. In terms of performance, the lateral actuators achieve sufficient deflection, even under high load conditions, using imitation human skin as the contact material and with a weight of 50 g. It is shown in a subject test that the lateral actuator works well under real conditions. A measurement of the combined movement has been performed using a Micro System Analyzer (MSA-100-3D) at different frequencies.

1. Introduction

Currently, users of a computer (PC) receive information acoustically and visually. They can control the PC with haptic inputs via mouse, keyboard or touchpad. With the proposed tactile display, we want to simulate real surface structure impressions in the fingertip of the user. Via the addition of an information transfer possibility and the use of the tactile stimuli of the user, our aim is that the PC can send tactile information back to the user.

There are four types of mechanoreceptors in the skin of the fingertip: the Merkel receptor, the Ruffini corpuscle, the Meissner corpuscle and the Pacinian corpuscle. Each is sensitive to specific stimuli. The Merkel receptor, also called SA-I (SA means slowly adapting), is a slowly adaptive receptor. It is stimulated with quasi static pressure vertical (normal) to the fingertip. The Ruffini corpuscle, called SA-II, is the second slowly adaptive receptor type. It is stimulated by skin

shearing. The Meissner corpuscle and the Pacini corpuscle are important for the proposed tactile display. They are also called RA-I and RA-II where RA means rapidly adapting. The Meissner corpuscle reacts to the excitation depending on the speed and the Pacini corpuscle reacts to the excitation depending on the acceleration [1–3]. According to [4–6], the SA-I receptors have their maximum sensitivity frequency range in the range of ~ 0.3 –100 Hz and the SA-II receptors in the range of ~ 7 –400 Hz. According to [7,4–6], the RA-I receptors have their maximum sensitivity frequency range in the range of ~ 3 –200 Hz and the RA-II receptors in the range of ~ 10 –800 Hz. The position of the individual receptors in the finger also influences sensation. However, the position of the receptors is not quite as important as the identifiability of the individual pins as such in this work. If the subject can identify the individual pins, the distance from pin center to pin center is too great. There are different approaches for the development of tactile displays. They can be classified into three stimulation types: the

[☆] This paper was recommended for publication by Pen-Cheng Wang.

* Corresponding author.

E-mail address: schmelt@ids.uni-hannover.de (A.S. Schmelt).

simulation of physical characteristics, the electrical activation of the mechanoreceptors, and the stimulation of the mechanoreceptors [8]. The focus of this paper is on the stimulation of the mechanoreceptors.

For development of the tactile display, it is important to know the load conditions of a tactile display. It has been shown that impedance measurements of the finger can be used for this purpose. These measurements have already been carried out by other researchers. In [9] an impedance curve is shown which was performed with a test pen. With only a few measuring points, the authors were able to show that there is a minimum in the range of 200–300 Hz. In [10], impedance measurements on the finger were performed with another system. In this case, the subjects did not have to hold a test pen, but had to place their fingers on an actuator. The contact surface was the fingertip. While this shows a similar course as in [9], some differences were also present which may be due to the other contact conditions. However, the authors were able to create a substitute model for their tactile actuator from the impedance measurements and use it for further work. In addition to the load conditions, it is important to know which performance is required as a minimum by the tactile display under the load conditions. Here, the tactile detection threshold has proved to be a useful measure of the required amplitude. If a tactile display is not able to reach the tactile detection threshold under load conditions, the subject will not feel anything. Tactile detection threshold measurements were performed by [9–11]. It was shown [9] that above a frequency of 100 Hz the tactile detection threshold is already below 1 μm and that, as with the impedance measurements, a minimum lies in the range of 200–300 Hz. Similar behavior was found in [10] and the authors were able to make a good prediction of the amplitude in which the tactile detection threshold was to be reached. This behavior is also shown in [11]. In addition, the authors were able to show that older subjects need larger amplitudes for detection. Furthermore, the frequency range can be mentioned as a development parameter for a vibro-tactile display. In [1], the required frequency range is specified with up to 1 kHz. It is shown in [12] that an optimal pin spacing is between 1 mm and 2 mm. The individual pin can no longer be assigned to an individual receptor with a distance greater than 2 mm. If the distance is less than 1 mm, adjacent pins are perceived as one pin.

In the past, various tactile displays were suggested. They worked with different actuator types to ensure the required deflection at different frequencies. For example, there are pneumatic tactile displays where small bubbles are deflected [13–15]. There are also phase change actuators in which a liquid is evaporated and thus a pneumatic pressure is used to deflect the actuators [16]. There are smart fluid actuators in which the deflection of the actuators is controlled electrically or magnetically via liquids [17,18]. There are polymer actuators that can be controlled thermally or electrically [19,20]. Piezoelectric actuators are also used for tactile displays. Piezoelectric bending actuators are proposed in [4,21–24] and piezostacks with a hydraulic amplification in [25,26]. Shape memory alloys (SMA) are used in [27,28]. Electrostatic force actuators are used in [29,30]. Electromagnetic power actuators are used in [31–33]. A dielectric elastomer actuator is proposed in [34] and a multimodal actuator for a flexible tactile display with normal and rotational excitation is proposed in [35]. Finally, there are thermal tactile displays such as in [36] and direct electrical stimulation of the receptors with displays such as in [37].

The tactile display in [31] generates a normal excitation to the finger and works up to a frequency of 800 Hz with a maximum free amplitude of 100 μm . The displays proposed in [22,4,24] for generating braille information already have a very good spatial resolution of only 1 mm and produce skin shearing in a wide frequency range. The flexible display with the multimodal actuators made of [35] could already work up to a frequency of 250 Hz with an actuator size of only $47.5 \times 12 \times 27 \text{ mm}$. One of the best known tactile displays is probably the Optacon [21], which transmits a translation of graphic information about photocells to piezoelectric bimorphs, which are then deflected according to the information. This leads to very good detection rates

after a corresponding training phase of the subjects. In [38], the authors used piezoelectric bimorphs to measure the quasi-static mechanical parameters of the fingertip in a test setup. To describe the results they used a second order linear viscoelastic material model, similar to [39]. However, this study was the first to investigate relaxation and creep in the living glabrous skin. In [40,41] the authors describe a further development of the tactile display with piezoelectric bending actuators presented in [24]. While [40] shows the functionality with a free excursion amplitude of up to 100 μm in a frequency range up to 250 Hz, [41] shows that the display is very well suited for the identification of two continuous lines. One is horizontal and the other diagonal to it. They received the best detection rate at their specified maximum voltage of 90 V. The system is very compact with an area of 150 cm^2 and a weight of 60 g.

All these approaches to tactile displays are already leading in the right direction. However, we suppose that if one wants to imitate real surfaces with a vibro-tactile display, one cannot avoid choosing a multimodal approach similar to that in [35] to activate the corresponding receptors. The innovation in our proposed tactile display is a combined actuator that can stimulate the fingertip with both normal and shear stimulation. To stimulate the SA receptors, it is equipped with an actuator called “normal actuator”, which is an electromagnetic force actuator used especially for low frequencies up to 150 Hz and normal excitation. In order to stimulate the RA receptors, it has an actuator called a “lateral actuator”, which is especially used for high frequencies up to 1 kHz and shear excitation. As already mentioned, piezoelectric bending actuators in the braille range performed well, which is why they are used for the shear actuators. The display presented here has been designed to create a distribution of stress and strain in the finger that corresponds to that which occurs when the finger is traversed over a defined surface. The display is not intended for direct reproduction of the surface properties of a surface, such as extending and retracting pins to generate braille. However, for the generation of a stress and strain distribution in the finger that corresponds to an extending or retracting pin. This should be realized over different frequencies, different excitation directions and deflection amplitudes, as shown in previous works with only one excitation direction, e.g. laterally in [24]. An analytical description of the finger under such loads is not explained here, but a replacement model from impedance measurements is created and used to ensure the functionality of the display. We assume that the bimodal excitation possibility can contribute to a better modelling of the stress and strain distribution in the finger. In [42] the authors show that a reference perception excitation perpendicular to the finger can also be obtained with a tangential excitation with less displacement but higher force. This shows that both normal and tangential excitation of the finger can result in the same feeling but it shows also that the actuators don't need the same force and displacement for the same feeling. We assume that the stress and strain field in the finger can be modelled better with a bimodal actuator. As already mentioned, an actuator distance of less than 1 mm is optimal to reproduce real surface structures. However, this results in the actuators having to be correspondingly small, which is only possible to a limited extent, since the required deflection or force must be achieved. With a second actuator coupled, the respective individual actuators could be designed to match a specific frequency range. For example, the normal actuator for low frequencies with a high deflection but small force, and the tangential actuator for high frequencies with a small deflection but high force. This could not only help to further reduce the size of the actuators, but also to transmit the signal to be transmitted in more detail to the finger.

Both types of actuators were assembled to form an actuator called “tactile generator”. In a field of 4×4 there are 16 tactile generators with a good resolution of 2.4 mm. We propose a load model designed using impedance measurements of the fingertip for the development of the lateral actuator. In our impedance measurements, we measured up to a frequency of 1 kHz and with a pin that has almost the same contact

geometry as the lateral actuator with a rectangular contact area of $0.8 \text{ mm} \times 1.5 \text{ mm}$.

With this load model, the lateral actuator is developed and optimized utilizing the Transfer Matrix Method (TMM) using the matrices given in [39]. In order to describe the movement of the lateral actuator in combination with the normal actuator in the optimization process, the boundary condition of the lateral actuator is adapted. The tactile representation is based on the solution of the optimization process.

The question regarding the proposed tactile display, especially regarding the lateral actuator, is: Can the needed deflection be achieved even under load? To address this, we will show the results of experiments with a weight of 50 g on a human skin imitation on the tactile display. We show tactile detection threshold measurements with the pin of the impedance measurement in lateral direction. We set this detection threshold as a measure and present the result of an experiment in which a subject uses the display to answer the question.

The work is specialized to the lateral actuator and to the influence of the combination with the normal actuator. In Section 2, the experimental setup is described. In Section 3, a description of the proposed load model for the fingertip at the top of the lateral actuator is presented. In Section 4, the optimization process of the lateral actuator to the proposed load model is described. In Section 5, the proposed display design is shown. The experimental results and the characterization are shown in Section 6. In Section 7, the results are discussed. Section 8 is the conclusion.

2. Experimental setup

In this section, the different experimental setups of this work are described. In Section 2.1, the experimental setups of the impedance measurement and the detection threshold measurement are presented. In Section 2.2, the experimental setups of the characterization process are shown.

2.1. Impedance measurement and detection threshold measurement of the fingertip

In order to measure the impedance of the fingertip and for the threshold measurements, the subject put their finger on a pin (Fig. 1). The pin is fixed at an impedance probe (Brüel&Kjær, Typ 8001) to measure the force and acceleration, which is connected with an LF charge amplifier (Typ 2628, Brüel&Kjær). The impedance probe is fixed at the shaker (Typ 4810 Brüel&Kjær). For a signal generation, a function generator (NI PXI-5402, 14 Bit 20 MHz FGEN) and a Power Amplifier (BAA 120 BEAK V1) are used. The current is measured with a current probe and a TCP A300 Tektronix amplifier. The voltage is measured with a 20 MHz Differential Probe (N2772A Hewlett Packard). The measuring signals are transmitted to a measuring board (NI PXI-5105, 12 Bit 60 MS/s Digitizer) and the shaker is fixed at a load cell (PW6DC3 10 KG, HBM). The measurement was done ten times at one

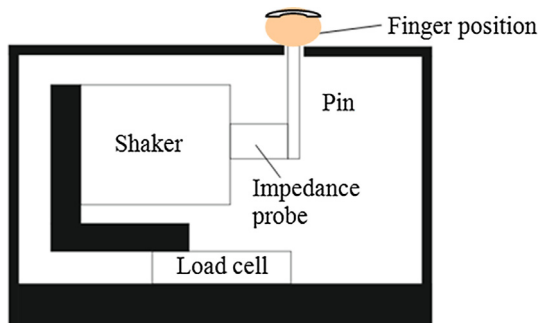


Fig. 1. Schematic representation of the experiment of the impedance and threshold measurement.

finger of one subject. The subject was encouraged to hold a constant preload of 2.5 g on the pin for the duration of the experiment. With the preload of 2.5 g for the threshold measurements and impedance measurements the individual pin were not surrounded too much by the fingertip, because in the later display the finger lies on several pins lying close together and thus cannot enclose the pin. An amplifier (AB22A MGCplus, HBM) is connected the load cell so the subject can see if they maintain the same preload on the pin for the time of measuring, and the actual force is additionally recorded. The pin has nearly the same top geometry as the lateral actuator with a rectangular contact area of $0.8 \text{ mm} \times 1.5 \text{ mm}$. The pin excites shearing at the fingertip, as does the lateral actuator. The excitation signal is a sine sweep from 10 Hz to 1000 Hz with a constant current amplitude (this leads to an approximate constant force amplitude) of 800 mA at the shaker. The results can be found in Section 3.

The same equipment is used for the threshold measurement, with a difference in the form of the excitation signal. A sine signal with different constant frequencies is used. The subjects place their finger on the pin and the amplitude of the excitation signal is increased until the subjects give a signal that they feel something. The amplitude is then reduced again until the subjects give a signal that they no longer feel anything. The mean value of the two amplitudes is then recorded as a threshold value. This experiment is performed with the frequency steps 10, 20, ..., 100, 150, ..., 300, 310, ..., 350, 400, 550 and 700 Hz. For this study, there were 12 subjects, aged of 24–30. There were 9 male and 3 female subjects. Only the average of all subjects is used. The results are used in the Sections 4 and 6.

2.2. Characterization of the tactile display

For the development of the tactile display, a first prototype tactile generator and a first prototype tactile display are used (see Section 5). A function generator (NI PXI-5402, 14 Bit 20 MHz FGEN) is used for the signal generation. The voltage is measured with a 20 MHz differential probe (N2772A Hewlett Packard). The measuring signals are transmitted to the measuring board (NI PXI-5105, 12 Bit 60 MS/s Digitizer). An Optic Fiber Vibrometer (OFV-552, Polytec) with a controller (OFV-5000, Polytec) with the decoder VD-09 is used to measure the velocity. The excitation signal is a sine sweep from 10 Hz to 2 kHz and an amplitude of 1 V. The application of 1 V is sufficient, because the experiment served to determine the support conditions of the lateral actuator. This is because linear spring and damper elements are assumed here. A schematic representation of the experiment is shown in Fig. 2. The results can be found in Section 6.

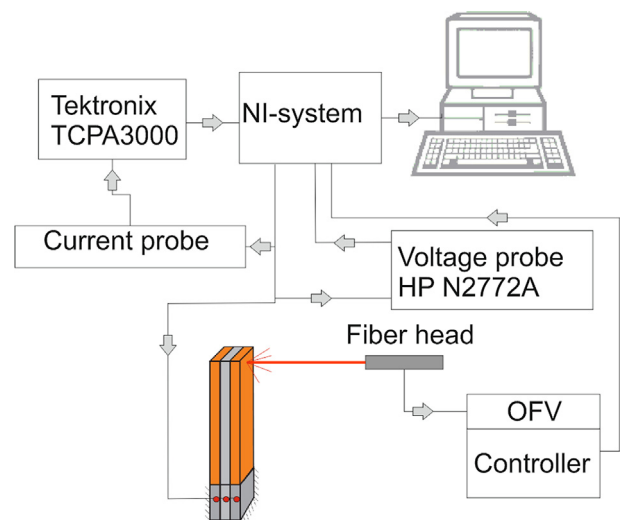


Fig. 2. Schematic representation of the experiment of the optimization process.

For the characterization of the lateral actuator as a part of the tactile generator (see Section 5.1), some experiments were performed. First, a measurement in a small signal range without load is made. The normal actuator is activated by a DC voltage with a current of 50 mA at the coil, so that the tactile generator is held firmly at its lower position. The next measurement is made with a non-activated normal actuator, so that the tactile generator is at its uppermost position. In both cases, the excitation signal at the lateral actuator is a sine sweep from 10 Hz to 1 kHz with an amplitude of 1 V. The voltage of 1 V is chosen because it is quite common to characterize piezo elements in this voltage range. If this experiment were carried out at higher voltages, the amplitude in the resonance frequency range could become so high that the lateral actuator would be destroyed. The second experiment will be a measurement in a large signal range under load condition. The load is a weight of 50 g on imitation human skin (made from the rubber of a crash dummy) at the top of the lateral actuator. The use of a 50 g weight or a preload of 50 g was perceived as pleasant in the emotional impression of the individual subjects and the skin imitation does not lose contact to the actuators with a preload of a weight of 50 g due to the movement of the actuator. The measurement is done as before in the two end positions of the tactile generator. The excitation signal at the lateral actuator for both positions is a sine sweep from 10 Hz to 1 kHz and with an amplitude of 50 V. The voltage 50 V was chosen because this voltage already ensures a tactile sensation with sufficiently large amplitudes. For these experiments, the same equipment as in the optimization process is used with one addition: the amplifier (HSA 4052, DC-500 kHz, NF) for the excitation signal of the lateral actuator. The results can be found in Section 6.

A time measurement will be performed for the characterization of the tactile generator with movements of both the normal and the lateral actuator, see Fig. 3. In the experiment, a 3D-laservibrometer (MSA-100-3D-M micro system analyzer Polytec) is used. The excitation signal of the lateral actuator is a sine wave with a constant frequency of 200 Hz and an amplitude of 10 V. The excitation signal of the normal actuator is a rectangular signal with a constant frequency of 100 Hz and a current amplitude of 120 mA. The results can be found in Section 6.

A performance test is carried out to determine a detection threshold measurement at the tactile display with one tactile generator. The display is placed on a scale, so that the subjects can keep a preload of



Fig. 3. MSA-100-3d-M Micro System Analyzer with a tactile display.

approximately 50 g on the display for the duration of the measurement. The other equipment used is the same as in the development process with the amplifier (HSA 4052, DC-500 kHz, NF). For this study, there were 10 subjects, aged of 24–30. All of them are male subjects. The excitation signal is a sine wave with different constant frequencies up to 1 kHz. The voltage amplitude is increased until the subjects feel the actuation. The results can be found in Section 6.

3. A load model of the finger on the lateral actuator

The impedance of the fingertip was measured to create a load model of the finger on the lateral actuator. The experiment is described in Section 2.1. In Fig. 4, the measured impedance and the measured phase can be seen. The grey lines are the ten measured signals of the subject. In the grey area between 300 Hz and 550 Hz the effect of the measurement equipment can be seen. Therefore, we didn't use this area for the evaluating. The behavior is due to the attached pin on the impedance probe. However, it can be assumed that the impedance of the finger has smoother course. The course of the impedance shows a similar behavior as in [9,10]. The differences are due to the different measurement methods. While a pen was used in [9] and a relatively large contact surface for the fingertip in [10], a pin was selected here whose contact geometry (with a rectangular contact area of 0.8 mm × 1.5 mm) is very similar to the contact geometry of the lateral actuator. Furthermore, the excitation direction had a substantial influence. Whereas in [9,10] the normal direction was excited, here only the lateral direction was excited.

The average of the amplitude of the impedance match good with a rational function and the average of the phase match good with a polynomial function in MATLAB (see Fig. 4, magenta lines). The fitting function of the amplitude of the impedance is $\hat{Z}(f)$ and of the phase $\varphi(f)$ are:

$$\hat{Z}(f) = \frac{p_1 \cdot f^2 + p_2 \cdot f + p_3}{f + p_4} \quad (1)$$

$$\varphi(f) = q_1 \cdot f^3 + q_2 \cdot f^2 + q_3 \cdot f + q_4 \quad (2)$$

The values are listed in Table 1:

The amplitude of the impedance and the phase can be combined to a complex number:

$$Z(f) = \hat{Z}(f) e^{j\varphi(f)} \quad (3)$$

Here j is the complex unit. This function is used to create a spring damper model (see Fig. 5), with the equations for the frequency depending stiffness and damping:

$$d(f) = \Re(Z(f)) \quad (4)$$

$$c(f) = -2\pi f \Im(Z(f)) \quad (5)$$

Here $d(f)$ is the damping, $c(f)$ the stiffness, \Re stands for the real part, \Im stands for the imaginary part and f the frequency. The stiffness and the damping are dependent on frequency (see Fig. 6). The stiffness has a maximum, as depicted in Fig. 6 left, near 900 Hz. The damping has a minimum in the range of 200 Hz–400 Hz.

4. Optimization of the lateral actuator

The development and the optimization process of the lateral actuator depend on the geometric boundaries of the display (see Section 5, Fig. 10). This includes soft support at the lower end of the lateral actuator by the normal force actuator and contact with the finger with the load model or without the finger at the upper end of the lateral actuator. The target is to obtain a spatial resolution smaller than 2.5 mm. Hence, the piezoelectric bimorphs of Johnson Matthey, with the properties listed in Table 2, are selected. The material with the

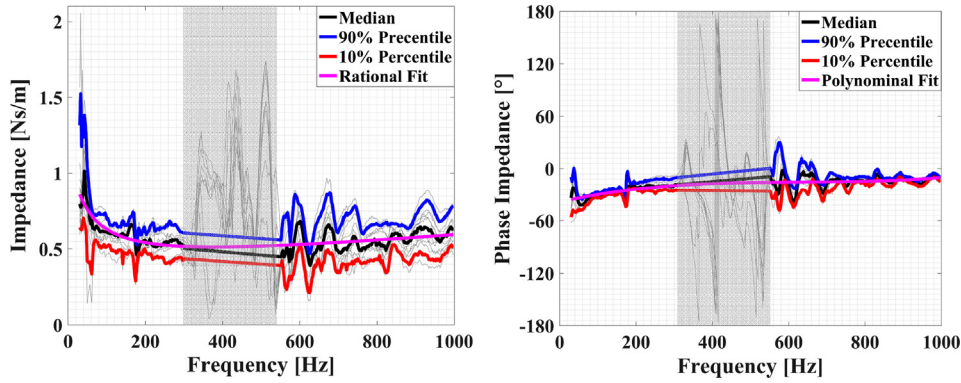


Fig. 4. Impedance and phase of the impedance of the fingertip with the 10%, 90% percentile and the average.

Table 1

Parameters of the fitting function of the impedance (left) and of the phase of the impedance (right).

p_1	$2.263e-4$	$[Ns^2/m]$	q_1	$8.327e-8$	$[s^3]$
p_2	$3.401e-1$	$[Ns/m]$	q_2	$-1.584e-4$	$[s^2]$
p_3	57.79	$[N/m]$	q_3	$1.036e-1$	$[s]$
p_4	49.17	$[1/s]$	q_4	-38.67	$[°]$

Table 2

Parameters of the piezoelectric bimorph.

Parameters		
Width	b	2.1 mm
Thickness of the piezo layers	h_p	0.26 mm
Thickness of the shim layer	h_s	0.25 mm
Density of the shim layer	ρ_s	1500 kg/m^3
Young's-modul of the shim layer	E_s	$1.4 \cdot 10^{11} \text{ N/m}^2$
Piezoceramic		"M1876"
Elastic compliance constant	s_{11}^E	$15.8 \cdot 10^{-12} \text{ m}^2/\text{N}$
Elastic compliance constant	s_{55}^E	$57.8 \cdot 10^{-12} \text{ m}^2/\text{N}$
Piezoelectric constant	d_{31}	$-385 \cdot 10^{-12} \text{ C/N}$

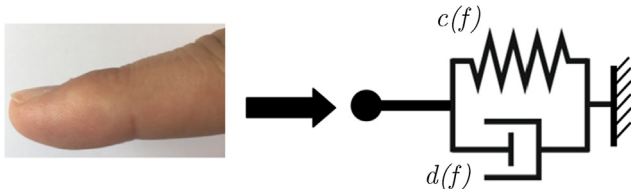


Fig. 5. Real finger (left), finger model (right).

largest absolute value of s_{55}^E , s_{11}^E and d_{31} by Johnson Matthey is chosen.

The thickness of the lateral actuators is determined by the material thickness of Johnson Matthey's commercial bimorphs. The width is optimally matched to the installation dimensions and the target spatial resolution of less than 2.5 mm. The parameter that can be varied is the length. This is done by using the theory of TMM like presented in [43] with using the model from Fig. 7. The calculation is done by our solver "Beks", a semi-analytical calculation. The mean value of the detection threshold measurement is used as a measure of the required deflection. The aim is to be as close to the threshold as possible or above it.

The equation system for the model consists of three matrices. The first matrix R_m for the support model, the second matrix A is for the bimorph and the third one is the matrix L_m for the load model of the fingertip. The matrix R_m results from the infinitesimally small section of the bimorph from 1 to 2:

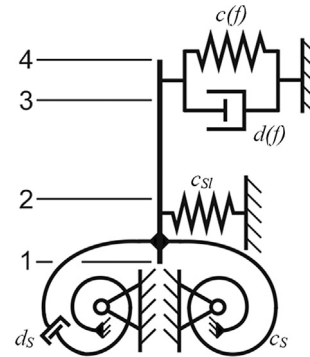


Fig. 7. Model of the tactile generator to optimize the length of the lateral actuator, with the load model as a spring and damper at the top of the lateral actuator. The support of the normal actuator is modeled as a spring, torsion spring, torsion damper and a mass moment of inertia at the lower side.

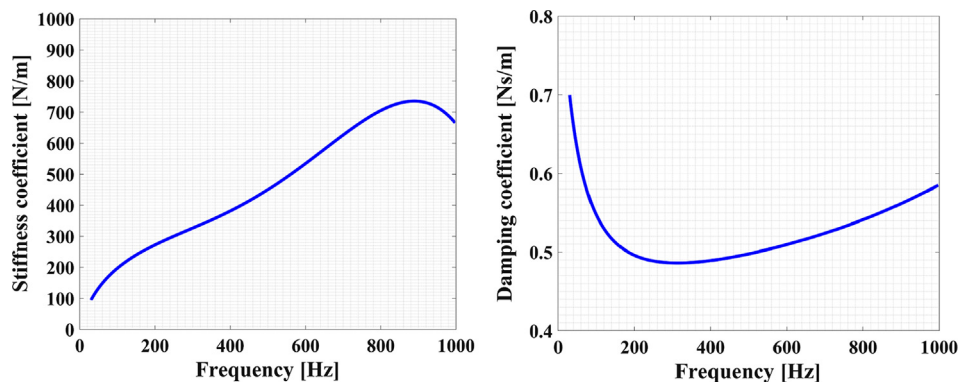


Fig. 6. Frequency dependent stiffness and damping coefficient.

$$\begin{bmatrix} v_2 \\ \dot{\psi}_2 \\ M_2 \\ F_2 \end{bmatrix} = \begin{bmatrix} 1 & 0 & 0 & 0 \\ 0 & 1 & 0 & 0 \\ 0 & R_{32} & 1 & 0 \\ R_{41} & 0 & 0 & 1 \end{bmatrix} \begin{bmatrix} v_1 \\ \dot{\psi}_1 \\ M_1 \\ F_1 \end{bmatrix} = \mathbf{R}_m \cdot \begin{bmatrix} v_1 \\ \dot{\psi}_1 \\ M_1 \\ F_1 \end{bmatrix} \quad (6)$$

$$R_{41} = \frac{c_{sl}}{j\Omega} \quad (7)$$

$$R_{32} = j\Omega\theta + d_s + \frac{c_s}{j\Omega} \quad (8)$$

Here c_{sl} is the stiffness of the spring, θ is the mass moment of inertia of the normal actuator, d_s is the damping of the torsion damper, c_s is the stiffness of the torsion spring, j is the complex unit and Ω is the angular frequency. The piezoelectric bimorph is modeled as a piezoelectric timoshenko beam based on the matrix \mathbf{A} of [39] from 2 to 3:

$$\begin{bmatrix} v_3 \\ \dot{\psi}_3 \\ M_3 \\ F_3 \\ U \end{bmatrix} = \begin{bmatrix} A_{11} & A_{12} & A_{13} & A_{14} & A_{15} \\ A_{21} & A_{22} & A_{23} & A_{24} & A_{25} \\ A_{31} & A_{32} & A_{33} & A_{34} & A_{35} \\ A_{41} & A_{42} & A_{43} & A_{44} & A_{45} \\ A_{51} & A_{52} & A_{53} & A_{54} & A_{55} \end{bmatrix} \begin{bmatrix} v_2 \\ \dot{\psi}_2 \\ M_2 \\ F_2 \\ U \end{bmatrix} = \mathbf{A} \cdot \begin{bmatrix} v_2 \\ \dot{\psi}_2 \\ M_2 \\ F_2 \\ U \end{bmatrix} \quad (9)$$

For a more detailed view of the elements in matrix \mathbf{A} , please refer to [Appendix A](#). The matrix \mathbf{L}_m for the infinitesimally small section from 3 to 4 results in:

$$\begin{bmatrix} v_4 \\ \dot{\psi}_4 \\ M_4 \\ F \end{bmatrix} = \begin{bmatrix} 1 & 0 & 0 & 0 \\ 0 & 1 & 0 & 0 \\ 0 & 0 & 1 & 0 \\ L_{41} & 0 & 0 & 1 \end{bmatrix} \begin{bmatrix} v_3 \\ \dot{\psi}_3 \\ M_3 \\ F_3 \end{bmatrix} = \mathbf{L}_m \cdot \begin{bmatrix} v_3 \\ \dot{\psi}_3 \\ M_3 \\ F_3 \end{bmatrix} \quad (10)$$

$$L_{41} = d(f) + \frac{c(f)}{j\Omega} \quad (11)$$

The system of equations for the model selected here thus results in:

$$\begin{bmatrix} v_4 \\ \dot{\psi}_4 \\ M_4 \\ F_4 \\ I \end{bmatrix} = \begin{bmatrix} & & & 0 \\ & & & 0 \\ & & & 0 \\ & & & 0 \\ 0 & 0 & 0 & 1 \end{bmatrix} \cdot \mathbf{A} \cdot \begin{bmatrix} v_1 \\ \dot{\psi}_1 \\ M_1 \\ F_1 \\ U \end{bmatrix} = \begin{bmatrix} & & & 0 \\ & & & 0 \\ & & & 0 \\ & & & 0 \\ 0 & 0 & 0 & 1 \end{bmatrix} \cdot \mathbf{R}_m \cdot \begin{bmatrix} v_1 \\ \dot{\psi}_1 \\ M_1 \\ F_1 \\ U \end{bmatrix} \quad (12)$$

In the first step, the parameters of the support condition are determined. For this purpose, a prototype of the tactile generator (see [Section 5](#), [Fig. 10](#)) is built in a prototype of the tactile display. The lateral actuator has a length of 14 mm. It is operated without load with a voltage amplitude of 1 V. The model is then adapted according to the available parameters so that a good match between model and experiment is achieved. The comparison of experiment to modeling can be seen in [Fig. 8](#). The boundary conditions for the calculation are: $F_1 = 0$, $M_1 = 0$, $M_3 = 0$, $F_3 = 0$ and $U = 1$ V. The values of the load model depending on the free movement of the lateral actuator is set to: $d(f) = 0$ and $c(f) = 0$.

The parameters for the support condition were empirically determined. The stiffness of the torsion spring is $c_s = 0.24$ Nm, the stiffness of the spring is $c_{sl} = 3 \cdot 10^6$ Nm, the damping coefficient of the torsion damper is $d_s = 4.46 \cdot 10^{-6}$ kg m²/s and the mass moment of inertia is $\theta = 1 \cdot 10^{-12}$ kg m². It is depicted in [Fig. 8](#) that the simulation and measurement are nearly the same in the frequency range up to 1 kHz.

After determining the support parameters, the model is calculated under load conditions in total for different lengths of the lateral actuator. The boundary conditions for the calculation are: $F_1 = 0$, $M_1 = 0$, $M_4 = 0$, $F_4 = 0$ and $U = 50$ V. [Fig. 9](#) shows the result of the simulation. It is shown that as the length of the lateral actuator increases, a minimum is shifted to lower frequencies. In this frequency range, however, a minimum should be avoided if possible, so that a sufficient amplitude can be achieved at these frequencies later on. The aim is not only to be located in a wide frequency range above or near the

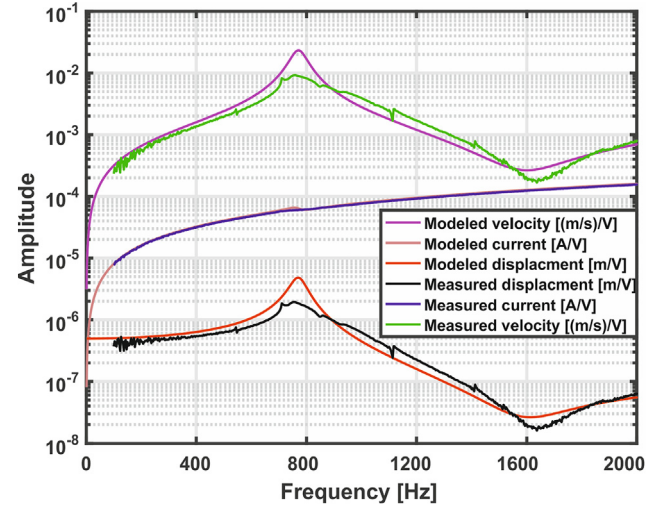


Fig. 8. Comparison of the measured and modeled behavior of the actuator.

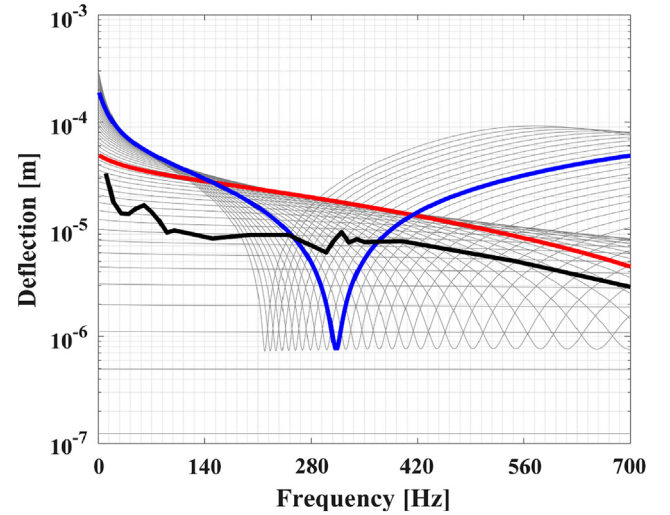


Fig. 9. Deflection amplitude of the lateral actuator over frequency. Each line represents a length of the lateral actuator. The red line represents the lateral actuator with a length of 20 mm and the blue line represents the lateral actuator with a length of 40 mm. The black line is the previously measured threshold value. (For interpretation of the references to color in this figure legend, the reader is referred to the web version of this article.)

threshold value measurement, but also to obtain an actuator that is as compact as possible. Therefore, a length of 20 mm is a good solution (see [Fig. 9](#), red line).

5. Design of the tactile display

In [Section 5.1](#), the design of the tactile generator is described with its coupling of the lateral actuator and the normal actuator. The design of the bimodal tactile display with 16 tactile generators is described in [Section 5.2](#).

5.1. Design of the tactile generator

The tactile generator is a coupled actuator (see [Fig. 10](#)). It consists of the lateral actuator and the normal actuator [44]. The normal actuator used in this tactile display acts as support of the piezo actuator, which is fixed (glued) at its top. In order to achieve a spatial resolution of 2.4 mm, the normal actuator is realized in a cylindrical shape with an outer diameter of 2.3 mm. It is driven electromagnetically using the

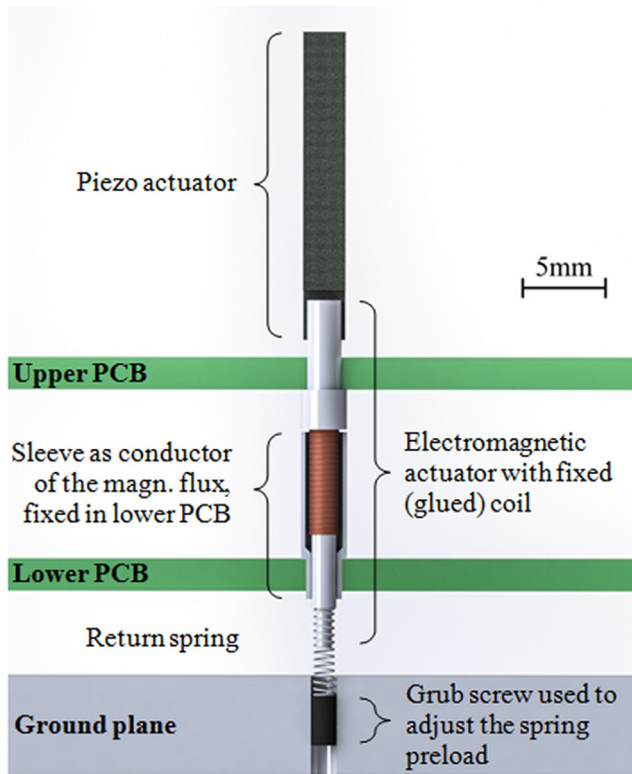


Fig. 10. The tactile generator [44].

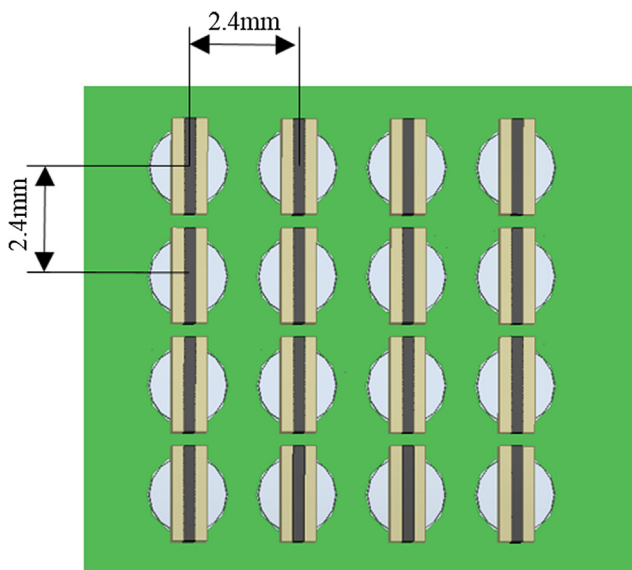


Fig. 11. Part of the top view of the CAD-model of the tactile Display to illustrate the spatial resolution.

reluctance principle. In contrast to the Lorentz principle, an electrical conductor placed in a magnetic field and forced to move analog to a current driven in the conductor is not needed. This way, a smaller design is possible or, in other words, in the same amount of space a higher force can be achieved. The coil fixed to the centered rod induces a magnetic flux that is led through the rod, crosses a small air gap of approximately $200\ \mu\text{m}$ and is then led through the outer sleeve fixed in a printed circuit board (PCB) and through another parasitic air gap back into the rod. The magnetic resistance of this magnetic circuit is lowered by minimizing the upper air gap. This is why the force resulting from

the reluctance principle always pulls the actuated rod towards the sleeve, regardless of the direction of the current. Therefore, a return spring is needed in order to push the rod back up when no current is applied to the coil. Another (upper) PCB works as a limiter for the way of travel of the normal force actuator. Its distance to the lower PCB is fixed but can be varied to change the size of the working air gap. The preload force of each spring can be varied by grub screws in the ground plate, which consists of non-conductive POM. As a result, the preload force can be set individually for each actuator and thus compensates for partial manufacturing-tolerance-related deviations.

The force applied to the finger is equal to the force of the spring minus the electromagnetic force and can reach $110\ \text{mN}$ with an air gap of $200\ \mu\text{m}$. A current of approximately $130\ \text{mA}$ is needed to pull the actuator down in this setup. When lowering the size of the air gap, the needed current decreases accordingly. The total actuator height of the normal and lateral actuator is $41\ \text{mm}$.

5.2. The tactile display

The tactile display consists of a lower circuit board in which 16 normal actuators are installed (see Fig. 12a)). The wires of the coils are soldered directly to the board. The board is connected to an upper board with spacers and springs on the spacers (see Fig. 12b)). The springs serve as an adjustment option for the movement of the normal actuators. The top board is attached to the ground plane with spacers. The lateral actuators are connected to the normal actuators. The cabling of the lateral actuators is then soldered to the upper circuit board. From the base plate, spacers for the support plate of the fingers are placed. Thus, the display has an area of $50\ \text{mm} \times 70\ \text{mm}$ and a total height of $45\ \text{mm}$. The spatial resolution is $2.4\ \text{mm}$ (see Fig. 11). Because each tactile generator has a footprint of no more than $2.3\ \text{mm} \times 2.3\ \text{mm}$, the tactile display can be extended to a larger surface area simply by adding more tactile generators. However, care must be taken regarding the guidance of the electric connections. More tactile generators result in a more complex printed circuit board.

6. Characterization and experimental results of the tactile display

The biasing force of the springs has an effect not only on the force of the normal actuator but also on the boundary condition of the lateral actuators. Thus, the adjustment of the admittance of the lateral actuator with its resonance frequency is possible within a range of $\sim 300\ \text{Hz}$. Hence, at the beginning of the characterization, all actuators are adjusted with the biasing force of the springs in the ground plane so that the resonance frequency of the lateral actuators are nearly at the same frequency. For the measurement of the display, an imitation skin and a $50\ \text{g}$ weight were placed at the top of the lateral actuators. The measurements are carried out with $1\ \text{V}$ voltage amplitude. This is to be understood as preparation for characterization.

After preparation, the measurement is carried out in the small signal range with the two end positions of the tactile generator as described in Section 2.2. To do this, the OFV (Optic Fibre Vibrometer) measures at the upper end of a tactile generator as shown in Fig. 13 on the left.

The measurement results show that some non-linear effects are present in the first position (see Fig. 14, left). There are left side overhanging frequency response characteristics. This is due to the possible movement of the tactile generator in its mounting. The tactile generator is pushed upwards by the spring, and if the movement of the lateral actuator is strong enough the contact loosens and friction or relative movement of the tactile generator occurs in its bearing. The bearing becomes softer and this is depicted in a softened stiffness with the curves overhanging to the left.

In the second position with the permanently activated normal actuator (see Fig. 14, right), a characteristic overhanging to the left can also be seen. However, due to the stiffer support by the magnetic field, the last peak in Fig. 14 on the left disappears almost completely. This

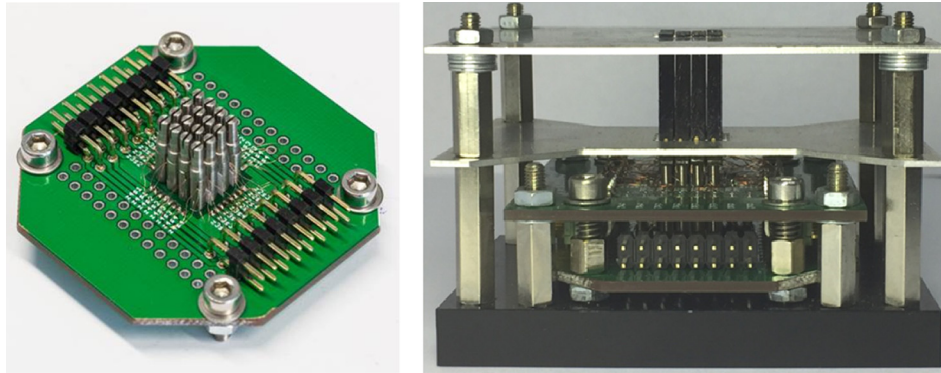


Fig. 12. (a) The lower circuit board with the normal actuators (left). (b) The tactile display (right).

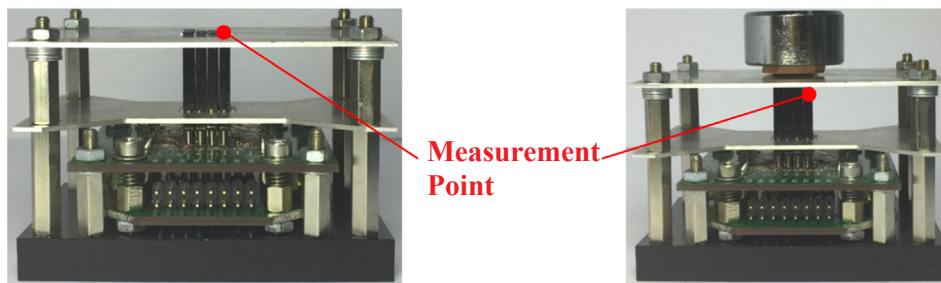


Fig. 13. Measurement position for the small signal measurement (left), the large signal measurement (right).

peak does not belong to the lateral actuator but comes from the combination with the normal actuator.

Measurements in the large signal range are performed in the same way in the small signal range, but with a voltage amplitude of 50 V and a non-free lateral actuator. A skin imitation and a 50 g weight are placed on the display. For reasons of space, the OFV (Optic Fibre Vibrometer) is adjusted under the support plate of the finger for the measurement of the velocities (see Fig. 13 right). In Fig. 15 left, the velocity, the current and the deflection of the lateral actuator with the non-actuated normal actuator is depicted. The previous measured detection threshold measurement (black line) is given for comparison. It is shown that the deflection is above the detection threshold measurement. If there is placed a fitting line for the displacement, it would have a slope of $1.164 \cdot 10^{-8}$ m/Hz over the measured frequencies. The values varies between $3.1 \cdot 10^{-6}$ and $2.48 \cdot 10^{-5}$ m. The deflection is also above the threshold measurement with the activated normal actuator (Fig. 15, right) and if there is placed a fitting line for the displacement, it would have a slope of $3.441 \cdot 10^{-8}$ m/Hz over the measured frequencies. The values varies between $1.36 \cdot 10^{-5}$ and $7.24 \cdot 10^{-5}$ m. For comparison, the simulated deflection from chapter 4 is inserted in brown. It can be seen that the simulated deflection and the measured deflection starts nearly at the same position and then the simulated deflection is below the measured course. This may be due to the different preload, when determining the simulated curve from the impedance measurement it was 2.5 g and in the measurement there was a 50 g weight on the lateral actuator. On the other hand, the difference can also come from the fact that there was no finger on the display, but the skin imitation.

Fig. 16 depicts the combined motion of the normal actuator and the lateral actuator in the time domain. These measurements are performed with the MSA-100-3D-M Micro System Analyzer. The orange line is the up and down movement, which is performed mainly by the normal actuator, and the blue¹ line is the movement of the lateral actuator.

¹ For interpretation of color in Fig. 16, the reader is referred to the web version of this article.

Fig. 16 shows that the movement of the normal actuator has an influence on the movement of the lateral actuator. The bearing condition changes with the motion of the normal actuator for the lateral actuator. The normal actuator is held firmly in the lower position by the magnetic field, at ~ 0 –3 ms. This is an almost firm boundary condition for the lateral actuator. In the range of 3–4 ms, the normal actuator is no longer activated and the spring pushes the actuator up again. At this point, it is for the lateral actuator like a free support, which significantly reduces the amplitude. In the range of 4–7 ms, the spring pushes the actuator back against the upper circuit board. Contact forces dissolve the free state and there is a stronger support for the lateral actuator again, but not as firm as with the activated magnetic field, which is shown by the reduced amplitude. The normal actuator is activated again from 7 ms to 9 ms. The applied magnetic field ensures a guided movement of the tactile generator downwards. This intermediate state is again a free state, but due to the guidance of the relatively strong magnetic field, this is a stronger support for the lateral actuator than when pushing it upwards, which can be seen from the greater amplitude. The process is then repeated. In a subjective test it turned out as expected that the sensation is different if only the lateral actuator or only the normal actuator or both are activated.

When the tactile detection threshold was tested with the new tactile display, the OFV (Optic Fiber Vibrometer) was aligned so that the laser dot measures at the same position as in Fig. 13 on the right. The subject put their finger on the display and the display was placed on a scale. The subject applied a preload of 50 g pressure on the display and hold. The right part of Fig. 17 shows the excitation voltage of the lateral actuator that was necessary for the subject to feel something. Furthermore, the deflection of the lateral actuator and the result of the previously measured detection threshold measurement can be seen in left part of Fig. 17.

It can be seen that the mean of all subjects starts at around $2 \mu\text{m}$ with an excitation voltage of ~ 8 V. It goes down up to $\sim 0.2 \mu\text{m}$ at 250 Hz. After, it slowly raises again, up to a frequency of 1000 Hz, up to a displacement of $\sim 1 \mu\text{m}$. The necessary excitation Voltage raises up to ~ 11 V at 100 Hz and after it goes down to ~ 3 V at 250 Hz. After it

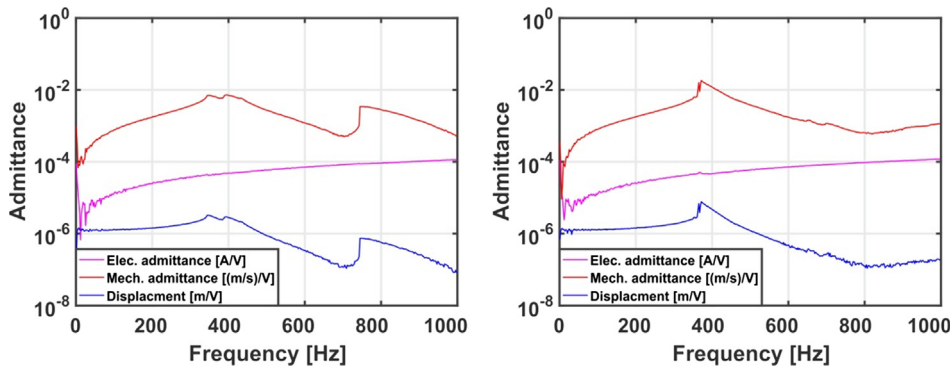


Fig. 14. Admittance of the lateral actuator with a non-actuated (left) and an activated normal actuator (right) in a small signal range of 1 V without load.

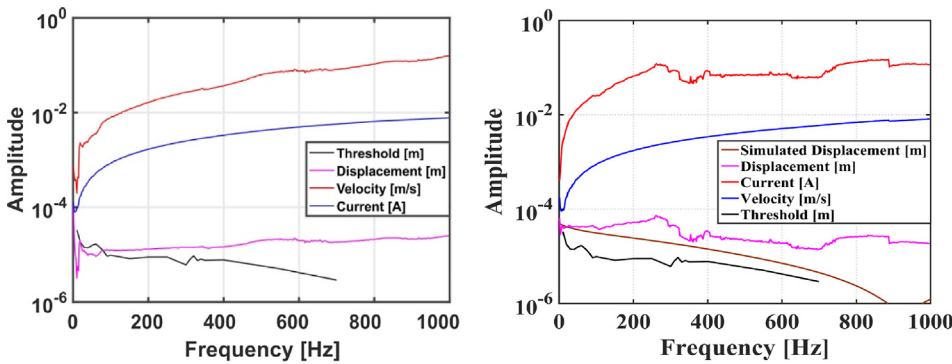


Fig. 15. Absolute values of the lateral actuator with a non-activated (left) and an activated normal actuator (right) in a large signal range of 50 V with load condition.

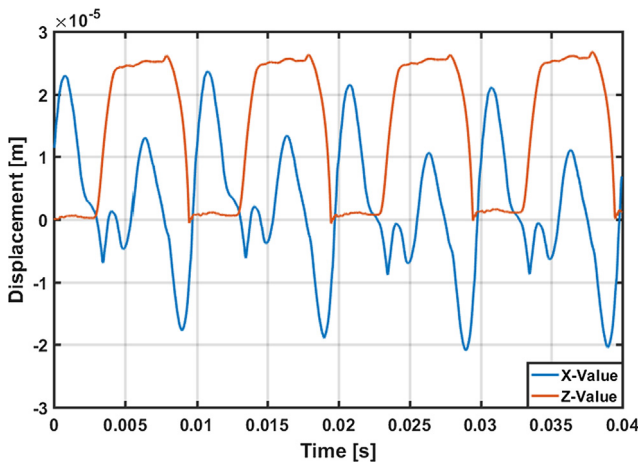


Fig. 16. Time response measurement with the MSA-100-3D-M of one actuator.

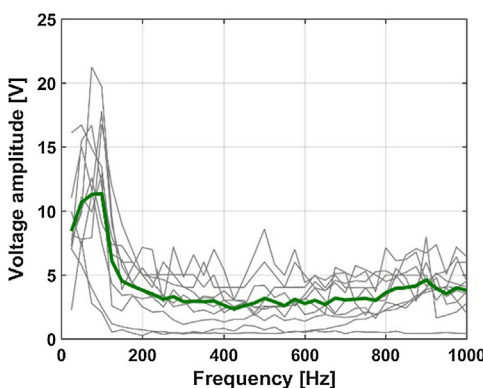
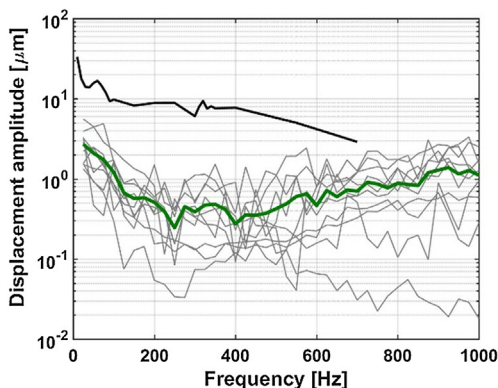


Fig. 17. Comparison of the threshold measurements (gray lines for the subjects, green line as the mean of all subjects) with the previously measured detection threshold (black line) (left) with the excitation voltage amplitude of the lateral actuator (gray lines for the subjects, green line as the mean of all subjects) (right). (For interpretation of the references to color in this figure legend, the reader is referred to the web version of this article.)

varies between 2.5 V and 4 V up to 1000 Hz. The largest excitation voltage amplitude of all subjects is at ~ 75 Hz with ~ 22 V. It can also be seen that one subject seems to be a little more sensitive than the others. Its minimum value is $\sim 0.02 \mu\text{m}$.

7. Discussion

A substitute model was created for the loading of the lateral actuator by the human finger based on impedance measurements. This substitute model, which consists of a frequency-dependent spring-damper element, is suitable for the design of shear force actuators as used here as piezoelectric bimorphs. Due to the mechanical representation with the help of a spring-damper element, it can be adapted to mechanical replacement models of a corresponding actuator. The parameters determined for this load model, which are specified in Section 3, will allow future developments of tactile displays to take actual load conditions during the design phase into account without having to carry out impedance measurements beforehand.

Based on this model, it has been shown that the human finger has no constant stiffness and damping properties. These values vary greatly depending on the frequency range. Fig. 6 shows that at very low frequencies below ~ 100 Hz only a very low stiffness (100 N/m) is present. While the stiffness at ~ 900 Hz has a maximum of ~ 750 N/m, the damping seems to behave like a Rayleigh damping. It starts at low frequencies at about 0.7 Ns/m with a minimum between 200 Hz and 400 Hz and a nearly constant increase thereafter. In order to create a model that can be used as a whole, further studies of subjects are indispensable. More studies should be conducted with subjects of different professions. A construction worker will surely have different values than an office worker, because of the calloused skin of their fingers. A significant advance would be made if a mechanical replacement model is found which combines stiffness and damping values for all three stress co-ordinate axes. Another important point is the impedance of the finger when it is on several actuators. This is because several actuators would probably lead to a different stress and strain behavior in the finger, which would probably change the impedance. This is an exciting point for future investigations.

It has been shown that the support of the lateral actuator has a considerable influence on the results. A first prototype of the tactile generator was built into a prototype display and its behavior was measured. Based on these results, the transfer matrix model (TMM) was adapted to take into account the specific storage conditions of the storage. The lateral actuator geometry was determined from this model. Due to the manufacturing tolerances of the individual actuators, especially the normal actuators and their gap dimensions, the optimization model is conditionally suitable for use on the tactile display. The preload force of the springs on the normal actuator causes a change in the support conditions of the lateral actuator and is therefore very difficult to integrate into the model for each individual lateral actuator.

In this description, it has been shown, particularly in the small signal range, that the connection of the normal actuator to the lateral actuator has a considerable effect on its behavior. Thus, a nonlinear behavior of the admittance curve was shown. The position of the normal actuator also has an influence on this behavior. In the loaded case, this influence was also shown in the large signal range at 50 V. However, it could be shown that the lateral actuator in both positions of the normal actuator generate the necessary deflection in order to achieve a tactile impression. The lateral actuators can work up to 230 V and thus a good tactile perception can be achieved with the correct control. Especially in the loaded case, an almost constant deflection of the lateral actuator was observed over the entire frequency range up to 1 kHz. The influence of the normal actuator on the lateral actuator is clearly visible from the time domain measurement. It was shown that the boundary condition of the lateral actuator changes with the motion of the normal actuator. It is thus apparent from this fact that better guidance of the normal actuator will have a positive effect on the movement of the lateral actuator.

In the experiment with skin imitation, it has been shown that the

Appendix A

The individual entries in Matrix A describing the piezoelectric timoshenko beam are:

$$A_{11} = C_0 - \sigma C_2 \quad (13)$$

$$A_{12} = -l(C_1 - (\sigma + \tau)C_3) \quad (14)$$

$$A_{21} = \frac{-\beta^4}{l} C_3 \quad (15)$$

$$A_{22} = C_0 - \tau C_2 \quad (16)$$

$$A_{31} = \frac{-\beta^4 C_2}{j\Omega a} \quad (17)$$

lateral actuator is able to achieve the deflection necessary in order to surpass the threshold measurement (see Fig. 15). In a subsequent experiment with 10 subjects, it was also possible to show that they could already feel something below the mean value of the previous measured perception threshold of Section 2.1. This may be due to the different preload of the experiments. A preload of only 2.5 g was applied for the threshold measurement, which served as a standard, and a preload of 50 g was applied during the test with the display. But this also shows that the subjects already feel something under an excitation voltage of 50 V. The difference between the perception thresholds is also certainly due to the number of subjects and thus the statistical deviation. But also the somewhat different contact conditions have their influence. At the threshold value measured before, the tests were carried out with only one pin. During the test with the display, only one actuator was controlled, but the other actuators served as support surface for the finger. Also the slightly different contact geometry of the actuator and the pin from the previously measured threshold experiment differed slightly, which also has an influence. Furthermore, the mean of all subjects starts at around $2 \mu\text{m}$ with an excitation voltage of ~ 8 V. It goes down up to $\sim 0.2 \mu\text{m}$ at 250 Hz. After, it slowly raises again, up to a frequency of 1000 Hz, up to a displacement of $\sim 1 \mu\text{m}$. This behavior suggests that mainly the Pacini corpuscle and the Meissner corpuscle were stimulated. For the two other mechanoreceptors, the amplitude is too small for these frequency, see [1–3].

8. Conclusion

To conclude, it can be said that our developed tactile display with combined actuators for normal and shear force excitation of the finger achieved a spatial resolution of 2.4 mm. The display can also be easily extended by adding additional actuators. We have shown that the finger has an influence on the actuators that cannot be neglected. A replacement model was created using impedance measurements and this was taken into account in the development process. Furthermore, we have shown with our lateral actuators that they are able to generate enough amplitude of movement to create a sensation up to a frequency of 1 kHz. This was shown in an experiment with a weight of 50 g on a skin imitation and in the measurement with subject. We assume that the bimodal excitation possibility can contribute to a better modelling of the stress and strain distribution in the finger. However, this must be evaluated in future studies.

Funding

The work was supported by the German Research Foundation (DFG-Project number: 224743555).

Conflict of interest

The authors declared that there is no conflict of interest.

$$A_{32} = \frac{l}{j\Omega a}(-\tau C_1 + (\beta^4 + \tau^2)C_3) \tag{18}$$

$$A_{41} = \frac{-\beta^4(C_1 - \sigma C_3)}{j\Omega a l} \tag{19}$$

$$A_{42} = \frac{\beta^4 C_2}{j\Omega a} \tag{20}$$

$$A_{51} = \frac{K}{l}(-\beta^4 C_3 + \sigma(-C_1 + C_4 + C_3(\sigma + \tau))) \tag{21}$$

$$A_{52} = K(C_5 - 1 + C_2 \sigma) \tag{22}$$

$$A_{13} = -j\Omega a C_2 \tag{23}$$

$$A_{14} = \frac{-j\Omega a l C_3}{\beta^4}(-\sigma C_1 + C_3(\beta^4 + \sigma^2)) \tag{24}$$

$$A_{23} = j\Omega \frac{a}{l}(C_1 - \tau C_3) \tag{25}$$

$$A_{24} = j\Omega a C_2 \tag{26}$$

$$A_{33} = C_0 - \tau C_2 \tag{27}$$

$$A_{34} = l(C_1 - C_3(\sigma + \tau)) \tag{28}$$

$$A_{43} = \frac{\beta^4}{l} C_3 \tag{29}$$

$$A_{44} = C_0 - \sigma C_2 \tag{30}$$

$$A_{53} = \frac{j\Omega a K}{l}(C_4 + C_3 \sigma) \tag{31}$$

$$A_{54} = j\Omega a K C_2 \tag{32}$$

$$A_{15} = -j\Omega a K C_2 \tag{33}$$

$$A_{25} = j\Omega \frac{a K}{l}(C_4 + C_3 \sigma) \tag{34}$$

$$A_{35} = K(C_5 - 1 + C_2 \sigma) \tag{35}$$

$$A_{45} = \frac{-\beta^4}{l} K C_3 \tag{36}$$

$$A_{55} = j\Omega C_p k_{kl} + \frac{j\Omega}{l}(a K^2(C_4 + C_3 \sigma)) \tag{37}$$

Here is C_0 to C_5 and σ , τ , β , a , K with the eigenvalues of the timoshenko beam $\lambda_{1,2}$:

$$C_0 = \frac{(\lambda_2^2 \cosh(\lambda_1) + \lambda_1^2 \cos(\lambda_2))}{\lambda_1^2 + \lambda_2^2} \tag{38}$$

$$\sigma = \frac{\widehat{m}_{eff} \Omega^2 l^2}{(EI)_{eff}} \tag{39}$$

$$C_1 = \frac{\left(\frac{\lambda_2^2}{\lambda_1} \sinh(\lambda_1) + \frac{\lambda_1^2}{\lambda_2} \sin(\lambda_2)\right)}{\lambda_1^2 + \lambda_2^2} \tag{40}$$

$$\tau = \frac{(\rho I)_{eff} \Omega^2 l^2}{(GA)_{eff}} \tag{41}$$

$$C_2 = \frac{(\cosh(\lambda_1) - \cos(\lambda_2))}{\lambda_1^2 + \lambda_2^2} \tag{42}$$

$$\beta^4 = \frac{\widehat{m}_{eff} \Omega^2 l^4}{(EI)_{eff}} \tag{43}$$

$$C_3 = \frac{\left(\frac{1}{\lambda_1} \sinh(\lambda_1) - \frac{1}{\lambda_2} \sin(\lambda_2)\right)}{\lambda_1^2 + \lambda_2^2} \tag{44}$$

$$a = \frac{l^2}{(EI)_{eff}} \quad (45)$$

$$C_4 = \frac{(\lambda_1 \sinh(\lambda_1) + \lambda_2 \sin(\lambda_2))}{\lambda_1^2 + \lambda_2^2} \quad (46)$$

$$\lambda_{1,2} = \sqrt{\sqrt{\beta^4 + 0.25(\sigma - \tau)^2} \mp 0.5(\sigma - \tau)} \quad (47)$$

$$C_5 = \frac{(\lambda_1^2 \cosh(\lambda_1) + \lambda_2^2 \cos(\lambda_2))}{\lambda_1^2 + \lambda_2^2} \quad (48)$$

The effective value $(\rho I)_{eff}$ of the beam is related to the thickness of the intermediate layer h_s , the thickness of the individual piezo layers h_p , the width b and the densities of the intermediate layer ρ_s and of the individual piezo layers ρ_p :

$$(\rho I)_{eff} = \left(\rho_s b \frac{h_s^3}{12} + \rho_p b \frac{2}{3} \left(\left(h_p + \frac{h_s}{s} \right)^3 - \left(\frac{h_s}{2} \right)^3 \right) \right) \quad (49)$$

The product of $(AG)_{eff}$ is with the shear modulus G , the piezo constant s_{55}^E and the correction factor for shear stress k :

$$(AG)_{eff} = k^2 b \left(Gh_s + \frac{2h_p}{s_{55}^E} \right) \quad (50)$$

The product of $(EI)_{eff}$ is with the compliance of the intermediate layer s_{ES} and the compliance of the piezo layer s_{EP} :

$$(EI)_{eff} = b \left(\frac{h_s^3}{12s_{ES}} + \frac{2}{3s_{EP}} \left(\left(\frac{h_s}{2} + h_p \right)^3 - \left(\frac{h_s}{2} \right)^3 \right) \right) \quad (51)$$

The mechanical compliance of the piezo layer s_{EP} with the mechanical damping is with the piezo constant s_{11}^E and the Quality factor Q :

$$s_{EP} = \left(\frac{1}{s_{11}^E} \left(1 + j \frac{1}{Q} \right) \right)^{-1} \quad (52)$$

The mass \hat{m}_{eff} is:

$$\hat{m}_{eff} = b(\rho_s h_s + 2\rho_p h_p) \quad (53)$$

K is with the piezoelectric constant d_{31} :

$$K = b \frac{d_{31}}{s_{EP}} (h_s + h_p) \quad (54)$$

The Capacitance C_p is, with the length l , the dielectric constant ϵ^T and the dissipation factor $\tan(\delta)$:

$$C_p = \frac{2lb \left(\epsilon^T (1 + j \tan(\delta)) - \frac{d_{31}^2}{s_{EP}} \right)}{h_p} \quad (55)$$

The clamped length of the bimorph is considered with the factor k_{kl} . However, because the bimorph is only attached to its intermediate layer and not to its ceramics, it follows that $k_{kl} = 1$. For a more detailed description of the equations, please refer to [36].

References

- [1] T.A. Kern, M. Matysek, O. Meckel, J. Rausch, A. Rettig, A. Röse, S. Sindlinger, Entwicklung haptischer geräte, Ein einstieg für ingenieure, Springer, Berlin, 2009.
- [2] M. Zimmermann, Das somataviszerale sensorische system, in: R.F. Schmidt, G. Thews, F. Lang (Eds.), Physiologie des Menschen, 28th ed., Springer, Berlin, 2000, pp. 216–235.
- [3] C. Doerrer, Entwurf eines elektromechanischen systems für flexible konfigurierbare eingabefelder mit haptischer rückmeldung, Technical University Darmstadt, Darmstadt, 2003.
- [4] V. Lévesque, Virtual display of tactile graphics and braille by lateral skin deformation, McGill University, Montreal, 2009.
- [5] M. Germani, M. Mengoi, M. Peruzzini, Electro-tactile device for material texture simulation, Int. J. Adv. Manuf. Technol. 68 (2013) 2185–2203.
- [6] J. Dargahi, S. Najarian, Human tactile perception as a standard for artificial tactile sensing-a review, Int. J. Méd. Robot. Comput. Assis. Surg. 1 (2004) 23–35.
- [7] D. Fitzpatrick, The somatic sensory system, in: D. Purves, G.J. Augustine (Eds.), Neuroscience, third ed., Sinauer Associates Inc., USA, 2004, pp. 189–208.
- [8] H. Ishizuka, N. Miki, MEMS-based tactile displays, Displays 37 (2015) 25–32.
- [9] A. Israr, S. Choi, H.Z. Tan, Detection threshold and mechanical impedance of the hand in a pen-hold posture, Proc. 2006 IEEE/RSJ, 2006, pp. 472–477.
- [10] C. Hatzfeld, R. Werthschützky, Mechanical impedance as coupling parameter of force and deflection perception: Experimental evaluation, in: P. Isokoski, J. Springare (Eds.), EuroHaptics, Springer, Berlin, 2012, pp. 193–204.
- [11] G.A. Gescheider, S.J. Bolanowski, K.L. Hall, K.E. Hoffman, R.T. Verrillo, The effects of aging on information-processing channels in the sense of touch: I. Absolute sensitivity, Somatosens. Mot. Res. 11 (1994) 345–357.
- [12] S.J. Bensmala, J.C. Craig, T. Yoshioka, K.O. Johnson, SA1 and RA afferent response to static and vibrating gratings, Neurophysiology 95 (2006) 1771–1782.
- [13] X. Wu, S.-H. Kim, H. Zhu, C.-H. Ji, M.G. Allen, A refreshable braille cell based on pneumatic microbubble actuators, J. Microelectromech. Syst. 21 (2012) 908–916.
- [14] C.-H. King, M.O. Culjat, M.L. Franco, J.W. Bisley, E. Dutton, W.S. Grundfest, Optimization of a pneumatic balloon tactile display for robot-assisted surgery based on human perception, IEEE Trans. Biomed. Eng. 55 (2008) 2593–2600.
- [15] L. Santos-Carreras, K. Leuenberger, P. Rétornaz, R. Gasser, H. Bleuler, Design and psychophysical evaluation of a tactile pulse display for teleoperated artery palpation, Proc. 2010 IEEE/RSJ, 2010, pp. 18–22.
- [16] H.-J. Kwon, S.W. Lee, S.S. Lee, Braille dot display module with a PDMS membrane driven by a thermopneumatic actuator, Sens. Actuat. A: Phys. 154 (2009) 238–246.
- [17] T. Tsujita, M. Kobayashi, M. Nakano, Design and development of a braille display using micro actuators driven by ER suspension, Int. J. Appl. Electromagn. Mech. 33 (2010) 1661–1669.
- [18] T.-H. Yang, H.-J. Kwon, S.S. Lee, J. An, J.-H. Koo, S.-Y. Kim, D.-S. Kwon, Development of a miniature tunable stiffness display using MR fluids for haptic application, Sens. Actuat. A: Phys. 163 (2010) 180–190.
- [19] Y. Kato, T. Sekitani, M. Takamiya, M. Doi, K. Asaka, T. Sakurai, T. Someya, Sheet-type braille displays by integrating organic field-effect transistors and polymeric actuators, IEEE Trans. Electr. Dev. 54 (2007) 202–209.
- [20] G. Paschew, A. Richter, High-resolution tactile display operated by an integrated “Smart hydrogel” actuator array, Proc. SPIE, 2010, pp. 764234-1–764234-8.
- [21] J.G. Linvill, J.C. Bliss, A direct translation reading aid for the blind, Proc. IEEE 54 (1966) 40–51.
- [22] J. Pasquero, V. Hayward, STReSS: a practical tactile display system with one

- millimeter spatial resolution and 700Hz refresh rate, Proc. Eurohaptics, 2003, pp. 94–110.
- [23] P.M. Ros, V. Dante, L. Mesin, E. Petetti, P.D. Giudice, E. Pasero, A new dynamic tactile display for reconfigurable braille: Implementation and tests, *Front. Neuroeng.* 7 (2014) 1–13.
- [24] V. Lévesque, J. Pasquero, V. Hayward, Braille display by lateral skin deformation with the STReSS² tactile transducer, *Proc. World Haptics, 2007*, pp. 115–120.
- [25] J. Watanabe, H. Ishikawa, X. Aroutte, Y. Matusumoto, N. Miki, Artificial tactile feeling displayed by large displacement MEMS actuator arrays, *Proc. MEMS, 2012*, pp. 1129–1132.
- [26] T. Ninomiya, Y. Okayama, Y. Matsumoto, X. Arouette, K. Osawa, N. Miki, MEMS-based hydraulic displacement amplification mechanism with completely encapsulated liquid, *Sens. Actuat. A: Phys.* 166 (2011) 277–282.
- [27] T. Matsunaga, K. Totsu, M. Esashi, Y. Haga, Tactile display for 2-D and 3-D shape expression using SMA micro actuators, *Proc. 3rd Annu. International IEEE EMBS, 2005*, pp. 88–91.
- [28] R. Vitushinsky, S. Schmitz, A. Ludwig, Bistable thin-film shape memory actuators for applications in tactile displays, *J. Microelectromech. Syst.* 18 (2009) 186–194.
- [29] H. Sasaki, M. Shikida, K. Sato, A force transmission system based on a tulip-shaped electrostatic clutch for haptic display devices, *J. Micromech. Microeng.* (2006) 2673–2683.
- [30] S.Y. Kim, K.B. Kim, J. Kim, K.U. Kyung, A film-type vibrotactile actuator for hand-held device, *Hapt. Audio Interact. Des.* 7989 (2013) 109–116.
- [31] M. Benali-Khoudja, M. Hafez, A. Kheddar, VITAL: an electromagnetic integrated tactile display, *Displays* 28 (2007) 133–144.
- [32] S. Youn, D.G. Seo, Y.-H. Cho, A micro tactile transceiver for fingertip motion recognition and texture generation, *Sens. Actuat. A: Phys.* 195 (2013) 105–112c.
- [33] J. Streque, A. Talbi, P. Pernod, V. Preobrazhensky, New magnetic microactuator design based on PDMS elastomer and MEMS technologies for tactile display, *IEEE Trans. Hapt.* 3 (2010) 88–97.
- [34] H.S. Lee, H. Phung, D. Lee, U.K. Kim, C.T. Nguyen, H. Moon, J.C. Koo, J. Nam, H.R. Choi, Design analysis and fabrication of arrayed tactile display based on dielectric elastomer actuator, *Sens. Actuat. A: Phys.* 205 (2014) 191–198.
- [35] T. Li, H. Huang, J. Justiz, V.M. Koch, A miniature multimodal actuator for effective tactile feedback: design and characterization, *Proc. Eng.* 168 (2016) 1547–1550.
- [36] M. Arai, K. Terao, T. Suzuki, F. Simokawa, F. Oohira, H. Takao, Air-flow based multifunctional tactile display device with multi-jet integrated micro venturi nozzle array, *IEEE 25th International Conf. Micro Electro Mech. Systems (MEMS), 2012*, pp. 148–151.
- [37] K. Kitamura, N. Miki, Micro fabricated needle-arrays for stimulation of tactile receptors, *Proc. Eurohaptics, 2014*, pp. 552–558.
- [38] Q. Wang, V. Hayward, In vivo biomechanics of the fingerpad skin under local tangential traction, *J. Biomech.* 40 (2007) 851–860.
- [39] V. Hofmann, J. Twiefel, Optimization of a piezoelectric bending actuator for a tactile virtual reality display, *DE GRUYTER, Energy Harvest. Syst.* 2 (2015) 177–185.
- [40] Q. Wang, V. Hayward, Compact, portable, modular, high-performance, distributed tactile transducer device based on lateral skin deformation, *Symposium on Haptic Interfaces for Virtual Environment and Teleoperator Systems IEEE VR, 2006*, pp. 67–72.
- [41] Q. Wang, V. Hayward, Biomechanically optimized distributed tactile transducer based on lateral skin deformation, *Int. J. Robot. Res.* 29 (2010) 323–335.
- [42] J. Biggs, M.A. Srinivasan, Tangential versus normal displacements of skin: relative effectiveness for producing tactile sensations, *Symposium on Haptic Interfaces for Virtual Environment and Teleoperator Systems IEEE Computer Society, 2002*, pp. 121–128.
- [43] E.C. Pestel, F.A. Leckie, *Matrix Methods in Elasto Mechanics*, McGraw-Hill, New York, 1963.
- [44] E. Fischer, A. Glukhovskoy, A.S. Schmelt, J. Twiefel, M.C. Wurz, Mikroaktuatorik für ein taktiles display, *Proc. MikroSystemTechnik Kongress, 2017*, pp. 515–518.